

Tobacco aquaporin NtAQP1 is involved in mesophyll conductance to CO₂ *in vivo*

Jaume Flexas^{1,*}, †, Miquel Ribas-Carbó^{1,†}, David T. Hanson^{2,†}, Josefina Bota¹, Beate Otto³, Josep Cifre¹, Nate McDowell⁴, Hipólito Medrano¹ and Ralf Kaldenhoff³

¹Laboratori de Fisiologia Vegetal, Grup de Biologia de les Plantes en Condicions Mediterrànies, Universitat de les Illes Balears, Carretera de Valldemossa Km 7.5, 07122 Palma de Mallorca, Balears, Spain,

²University of New Mexico, Department of Biology, Albuquerque, NM 87131, USA,

³Darmstadt University of Technology, Institute of Botany, Applied Plant Sciences, Schnittspahnstrasse 10, D-64287 Darmstadt, Germany, and

⁴Los Alamos National Laboratory, Los Alamos, NM 87544, USA

Received 24 April 2006; revised 26 June 2006; accepted 17 July 2006.

*For correspondence (fax +34 971 17 3184; e-mail jaume.flexas@uib.es).

†These authors contributed equally to this work.

Summary

Leaf mesophyll conductance to CO₂ (g_m) has been recognized to be finite and variable, rapidly adapting to environmental conditions. The physiological basis for fast changes in g_m is poorly understood, but current reports suggest the involvement of protein-facilitated CO₂ diffusion across cell membranes. A good candidate for this could be the *Nicotiana tabacum* L. aquaporin NtAQP1, which was shown to increase membrane permeability to CO₂ in *Xenopus* oocytes. The objective of the present work was to evaluate its effect on the *in vivo* mesophyll conductance to CO₂, using plants either deficient in or overexpressing NtAQP1. Antisense plants deficient in NtAQP1 (AS) and NtAQP1 overexpressing tobacco plants (O) were compared with their respective wild-type (WT) genotypes (CAS and CO). Plants grown under optimum conditions showed different photosynthetic rates at saturating light, with a decrease of 13% in AS and an increase of 20% in O, compared with their respective controls. CO₂ response curves of photosynthesis also showed significant differences among genotypes. However, *in vitro* analysis demonstrated that these differences could not be attributed to alterations in Rubisco activity or ribulose-1,5-bisphosphate content. Analyses of chlorophyll fluorescence and on-line ¹³C discrimination indicated that the observed differences in net photosynthesis (A_N) among genotypes were due to different leaf mesophyll conductances to CO₂, which was estimated to be 30% lower in AS and 20% higher in O compared with their respective WT. These results provide evidence for the *in vivo* involvement of aquaporin NtAQP1 in mesophyll conductance to CO₂.

Keywords: aquaporins, *Nicotiana*, CO₂ permeability, photosynthesis, leaf conductance.

Introduction

Photosynthesis requires the diffusion of CO₂ from the atmosphere into the leaf and then to the site of carboxylation in the chloroplast stroma. The rate of fixation can be limited by the conductance of CO₂ into the leaf through stomata (g_s) and by the conductance from substomatal cavities through the leaf mesophyll to the chloroplast stroma (g_m). From Fick's law of diffusion, the net photosynthetic flux (A_N) can be expressed as: $A_N = g_s(C_a - C_i) = g_m(C_i - C_c)$, where C_a , C_i and C_c are the CO₂ concentrations ($\mu\text{mol mol}^{-1}$ air) in the atmosphere, the substomatal

cavity and the chloroplast stroma, respectively (Long and Bernacchi, 2003).

Gas exchange studies have usually assumed that g_m is large and constant, i.e. that $C_i \approx C_c$ (Farquhar *et al.*, 1980). However, there is now evidence that g_m may be sufficiently small so as to significantly decrease C_c relative to C_i , therefore limiting photosynthesis (von Caemmerer and Evans, 1991; Di Marco *et al.*, 1990; Evans and von Caemmerer, 1996; Evans and Loreto, 2000; Evans *et al.*, 1986; Harley *et al.*, 1992; Loreto *et al.*, 1992). Moreover, g_m is not

constant, since it has been shown to acclimate during leaf development (Hanba *et al.*, 2001; Miyazawa and Terashima, 2001) and senescence (Loreto *et al.*, 1994), as well as to light conditions during growth (Piel *et al.*, 2002) and CO₂ environments (Singsaas *et al.*, 2004). There is also evidence for rapid variation of g_m in response to drought (Brugnoli *et al.*, 1998; Flexas *et al.*, 2002; Roupsard *et al.*, 1996), salinity (Bongi and Loreto, 1989; Delfine *et al.*, 1998, 1999; Loreto *et al.*, 2003), changes in light intensity (JF and DTH, unpublished results), leaf temperature (Bernacchi *et al.*, 2002) and CO₂ concentration (Centritto *et al.*, 2003; Düring, 2003). With respect to CO₂ concentration, the response of g_m has been shown to be as rapid and reversible as that of g_s (Centritto *et al.*, 2003).

Despite substantial evidence for the large variability of g_m , the mechanism behind these variations remains unclear. Early literature assumed that structural properties of the leaf caused most variations in g_m (von Caemmerer and Evans, 1991; Lloyd *et al.*, 1992; Nobel, 1999). While structural properties could be involved in adaptive and acclimation responses, they could not account for the rapid variations observed in response to varying environmental conditions. Most likely, a metabolic process is involved changes in g_m in these cases. Based on a temperature response coefficient (Q_{10}) of approximately 2.2 for g_m in tobacco leaves, Bernacchi *et al.* (2002) speculated that enzymatic or protein-facilitated diffusion of CO₂ controls g_m . The most likely candidates for this effect would be carbonic anhydrase and aquaporins.

Some authors have suggested that the activity of carbonic anhydrase is closely associated with g_m in C₃ plants (Makino *et al.*, 1992; Sasaki *et al.*, 1996; Volokita *et al.*, 1983). However, modification of carbonic anhydrase activity revealed little or no change in g_m and photosynthesis (Price *et al.*, 1994; Williams *et al.*, 1996). Recently, Gillon and Yakir (2000) showed that the relative contribution of carbonic anhydrase to the overall g_m is species dependent. They hypothesized that carbonic anhydrase-mediated CO₂ diffusion may be more important when g_m is low due to structural properties of the leaves, as is the case for woody species, where cell wall conductance is much lower than chloroplast conductance. In mesophyte species, such as tobacco (*Nicotiana tabacum* L.), the influence of carbonic anhydrase in g_m seems negligible (Gillon and Yakir, 2000).

Aquaporins are water channel integral membrane proteins that increase the permeability of membranes to water, thus playing an essential role in plant water relations (Chrispeels *et al.*, 2001; Kaldenhoff *et al.*, 1998; Kjellbom *et al.*, 1999; Maurel and Chrispeels, 2001; Maurel *et al.*, 1993, 1997; Tyerman *et al.*, 2002). Some aquaporins also facilitate the membrane transport of other small, uncharged molecules, such as ammonia, boric acid, hydrogen peroxide, glycerol or urea, across membranes (Baiges *et al.*, 2002;

Beitz *et al.*, 2006; Biela *et al.*, 1999; Holm *et al.*, 2004; Jahn *et al.*, 2004; Liu *et al.*, 2003; Meinild *et al.*, 1998; Tyerman *et al.*, 2002). The hypothesis that aquaporins could be involved in regulation of g_m was motivated by the observation that oocytes expressing mammalian aquaporin 1 (AQP1) or NtAQP1 had increased permeability of the membrane to CO₂ (Cooper and Boron, 1998; Nakhoul *et al.*, 1998; Uehlein *et al.*, 2003). Until recently, the possibility that CO₂ may permeate aquaporins in plants had not been examined in detail (Tyerman *et al.*, 2002). The first indirect evidence was provided by Terashima and Ono (2002), who impaired mesophyll conductance to CO₂ using HgCl₂ (a non-specific inhibitor of some aquaporins). Hanba *et al.* (2004) showed that expressing the barley aquaporin HvPIP2;1, in transgenic rice leaves resulted in an increased g_m , though it also produced changes in leaf morphology.

NtAQP1 is a member of the plasma membrane aquaporin 1 family (PIP1), which is mercury-insensitive and permeable to water and glycerol, but impermeable to Na⁺, K⁺ and Cl⁻ (Biela *et al.*, 1999). While NtAQP1 is expressed preferentially in roots, it has been shown to be present in almost all organs of tobacco (Otto and Kaldenhoff, 2000). In leaves, NtAQP1 accumulates in cells of the spongy parenchyma, with the highest concentration around substomatal cavities (Otto and Kaldenhoff, 2000). Using antisense plants, Siefritz *et al.* (2002) demonstrated *in vivo* that NtAQP1 is involved in root cellular transport of water, root hydraulic conductivity and response of the whole plant to water stress. More recently, Uehlein *et al.* (2003) demonstrated that tobacco aquaporin NtAQP1 facilitates transmembrane CO₂ transport by expression in *Xenopus* oocytes. Transgenic NtAQP1 plants (antisense and induced overexpression) regulated stomatal conductance upon transferring leaves from darkness to light in a manner suggesting that NtAQP1 expression could be affecting g_m (Uehlein *et al.*, 2003). However, a direct analysis of the role of NtAQP1 in g_m *in vivo* is still not available. The objective of the present study was to determine g_m *in planta* using transgenic tobacco plants that differ in NtAQP1 expression by a combination of gas exchange, chlorophyll fluorescence and on-line ¹³C isotope discrimination techniques.

Results

Constitutive antisense (AS) plants were constructed from Samsun strains (CAS), while overexpressing plants (O) were constructed from Hö 20.20 strains (CO). NtAQP1 overexpression was under control of a tetracycline-inducible promoter. The presence of NtAQP1 was significantly reduced in AS plants compared with their control CAS, and significantly increased in O plants compared with their control CO 2 days after tetracycline application (Figure 1). These results are consistent with a previous analysis of RNA expression in the same lines (Uehlein *et al.*, 2003).

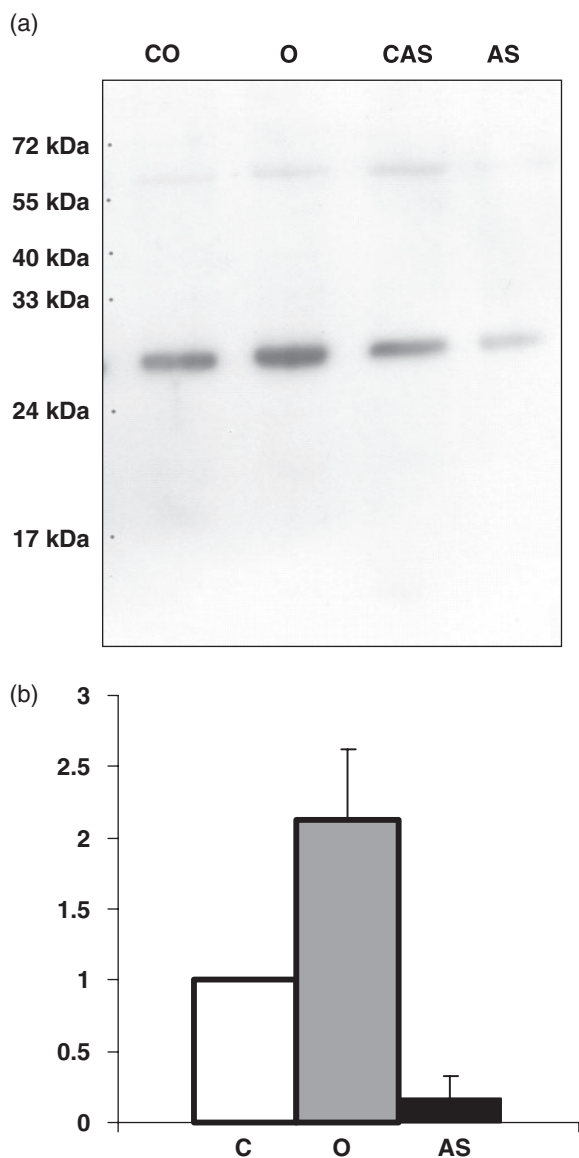


Figure 1. Relative NtAQP1 concentration.

(a) Equal amounts of leaf-protein from controls (CO, control overexpression; CAS, control antisense), overexpressing (O) and antisense (AS) plants were subjected to a Western analysis using an NtAQP1-specific antibody. The signal intensity at the size of the NtAQP1 monomeric protein was increased in O or decreased in AS protein preparations indicating improved and reduced expression of NtAQP1, respectively. Protein samples were obtained from pooled individual plants subjected to physiological analysis.

(b) Quantification of NtAQP1 protein from Western blot. Signal intensities from protein samples obtained from pooled CAS and CO controls (C, white column) were set as 1 and the data from NtAQP1 overexpressing lines (O, grey column) or NtAQP1 antisense lines (AS, black column) are given in relation to it. Values represent means of 30 independent plants from three lines (AS) or six plants from a single line (O). Standard deviation is indicated by bars.

Approximately 8 weeks after sowing, and despite having very different NtAQP1 contents, CAS, AS, CO and O plants were visually undistinguishable. Plant height, stem diameter, the number of leaves per plant and the mean leaf length

were very similar (Table 1). Although there were significant differences in leaf mass area and relative water content (RWC) between plants from the Samsun line and plants from the Hö 20.20 line, no differences were observed in general between control and transgenic plants. Only RWC was significantly lower in O compared with CO, but the difference was nevertheless small. Both AS and O plants had a similar surface area of mesophyll cells (S_m) and chloroplasts (S_c) exposed to intercellular air spaces per leaf area to their respective controls (Table 1).

Despite similarities in plant and leaf morphology, significant differences were observed among plant lines in photosynthetic function, particularly at near-saturating and saturating light intensities (Figure 2). The electron transport rate (J) was similar among plant lines (Figure 2a,b), but net CO₂ assimilation (A_N) was lower in AS than in CAS, and higher in O than in CO (Figure 2c,d). Gas exchange and fluorescence rates were identical in CO and O plants prior to the induction of overexpression of NtAQP1 by adding tetracycline (data not shown). Therefore, the differences observed in Figure 2 originated from tetracycline-induced gene expression of NtAQP1.

Furthermore, the response of J and A_N to varying substomatal CO₂ concentration (C_i) differed strongly between the plant lines (Figure 3). At high light intensities, J first increased in response to C_i in all lines, with maximum J at C_i around 400–600 $\mu\text{mol CO}_2 \text{ mol}^{-1}$ air (Figure 3a,b), and decreased thereafter. A similar response was described by Sharkey *et al.* (1988) under high light intensities, and it is thought to be caused by a feedback limitation from utilization of the end product. At any given C_i , J_{PSII} was lower in AS than in CAS, and higher in O than in CO. A_N - C_i curves showed similar trends (Figure 3c,d), with a clear limitation by triose-phosphate utilization (TPU) at high C_i in AS and CAS, as evidenced by a small decline of A_N with increasing C_i (Harley and Sharkey, 1991; Long and Bernacchi, 2003) that was not apparent in O and CO. Both the saturated rate and the initial slope (insets) of these curves were significantly lower in AS than in CAS, and significantly higher in O than in CO. Prior to application of tetracycline, no significant differences had been observed between CO and O plants in their A_N - C_i curves (Figure 4).

In total the data from both A_N -PFD (where PFD is the photosynthetically active photon flux density) and A_N - C_i curves, illustrate significant differences in A_N at a PFD of 1000 $\mu\text{mol m}^{-2} \text{ sec}^{-1}$ and C_a of 400 $\mu\text{mol CO}_2 \text{ mol}^{-1}$ among different plant lines (Table 2). The O plants displayed the highest values (21.9 $\mu\text{mol CO}_2 \text{ m}^{-2} \text{ sec}^{-1}$) and the AS plants the lowest (17.2 $\mu\text{mol CO}_2 \text{ m}^{-2} \text{ sec}^{-1}$), with the two control lines presenting middle values. Therefore, a difference of up to 21% was found in A_N between the two extreme lines. Similar differences were observed in stomatal conductance (g_s), so that A_N/g_s and C_i did not differ significantly among lines. In contrast to gas exchange parameters, the maximum

	CAS	AS	CO	O
Plant height (cm)	101 ± 3	95 ± 8	107 ± 3	102 ± 4
Stem diameter (mm)	19 ± 1	16 ± 1	20 ± 1	20 ± 1
No. leaves per plant	24 ± 2	27 ± 3	29 ± 2	25 ± 2
Leaf length (cm)	27.0 ± 0.6	24.5 ± 1.4	23.8 ± 0.6	22.3 ± 0.6
LMA (g m ⁻²)	25.7 ± 2.3	26.5 ± 2.2	39.5 ± 2.2	39.0 ± 1.8
S _m (m ² m ⁻²)	12.3 ± 1.1	12.4 ± 1.0	14.1 ± 0.6	13.4 ± 0.9
S _c (m ² m ⁻²)	9.1 ± 0.6	9.8 ± 1.1	10.5 ± 0.8	10.3 ± 0.6
RWC (%)	79.1 ± 1.4	75.8 ± 1.5	90.5 ± 0.7	86.6 ± 0.9*

Table 1 Morphological plant and leaf characteristics of the studied genotypes. Values are means ± SE of six replicates from independent plants per genotype

*Statistically significant ($P < 0.05$) difference between CAS and AS or between CO and O.

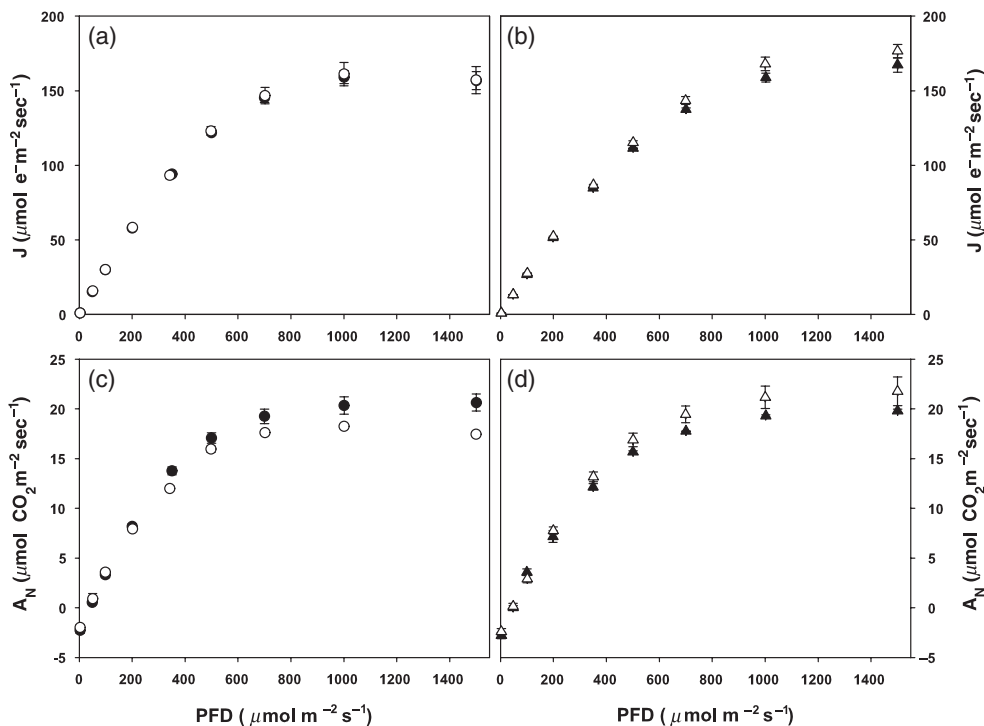


Figure 2. The response of the electron transport rate, J (a, b) and net photosynthesis, A_N (c, d) to incident light intensity, PFD, in (a, c) CAS (filled circles) and AS (empty circles) and (b, d) CO (filled triangles) and O (empty triangles). Values are means ± SE of six replicates from independent plants per genotype.

quantum yield of photosystem II (F_v/F_M) did not differ among lines (Table 2). Likewise, no significant differences were observed in carbonic anhydrase activity, amount or total activity of Rubisco, ribulose-1,5-bisphosphate (RuBP) content or the respiration rate in the dark (Table 2).

Estimations of g_m according to the methods of either Harley *et al.* (1992) or Terashima and Ono (2002) showed that, in general, the first method yielded somewhat higher values than the second (Table 2). However, both methods revealed proportionally similar important differences among plant lines. In AS plants, g_m was less than half that in O. Again, control lines showed intermediate values. As a consequence, the estimated CO₂ concentration in the chloroplasts differed among lines (Table 2). Prior to application of tetracycline, and according to the method by Terashima,

g_m averaged 0.330 ± 0.058 in CO and 0.335 ± 0.053 mol m⁻² sec⁻¹ in O.

These results were confirmed in two additional independent experiments, using two different techniques based on on-line ¹³C discrimination for g_m estimations (Table 3). The plants were grown under different conditions and with different ages at the time of measurement, depending on the experiments. This resulted in different values of A_N for each genotype (Tables 2 and 3). Despite the variation between treatments, it was clear that all methods for estimation of g_m generate values for AS plants that are 20–40% lower than CAS and 20–50% higher for O than for CO. Therefore, the g_m of O plants was around twice as large as that of AS. Last but not least, in all the experiments A_N and g_s changed proportionally to g_m .

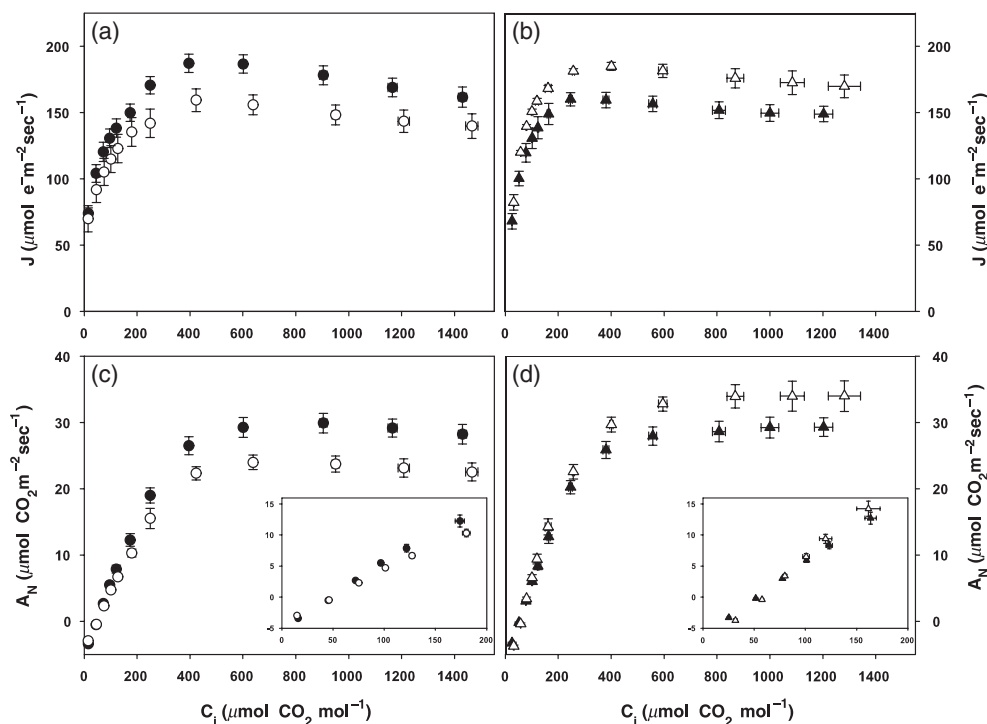


Figure 3. The response of the electron transport rate, J (a, b) and net photosynthesis, A_N (c, d) to substomatal CO₂ concentration, C_i , in CAS and AS (a, c) and CO and O (b, d). Values are means \pm SE of six replicates from independent plants per genotype. Insets in (c) and (d) amplify the initial slopes of the A_N - C_i curves. Symbols as in Figure 2.

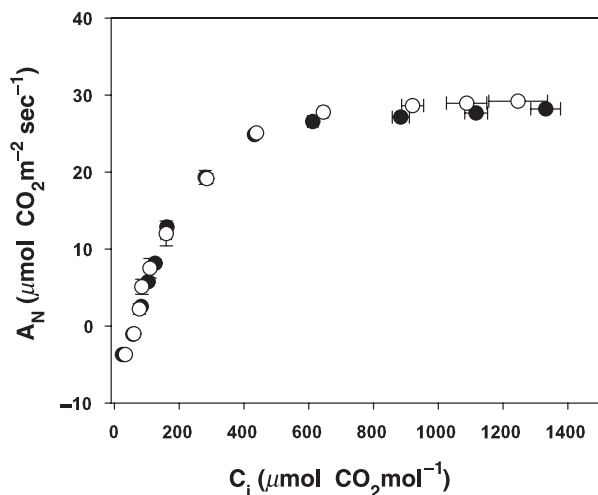


Figure 4. The response of net photosynthesis (A_N) to substomatal CO₂ concentration (C_i) in CO (filled symbols) and O plants (empty symbols) prior to tetracycline application. Values are means \pm SE of three replicates from independent plants per genotype.

Having an estimate of g_m allows simple conversion of A_N - C_i curves into response curves of A_N to chloroplast CO₂ concentration, C_c (Manter and Kerrigan, 2004). Using this method we found that differences among genotypes in the initial slope of A_N - C_i curves disappeared in A_N - C_c (Figure 5).

We then applied the equations of Farquhar *et al.* (1980) to the A_N - C_c curves shown in Figure 5 to estimate the maximum carboxylation capacities (V_{cmax}) which were identical ($145 \mu\text{mol m}^{-2} \text{sec}^{-1}$) in CAS, AS and CO plants, and somewhat higher ($160 \mu\text{mol m}^{-2} \text{sec}^{-1}$) in O plants. In contrast, the observed differences in light-saturated and CO₂-saturated rates persisted even in A_N - C_c curves (Figure 5). The maximum electron transport capacity (J_{max}) was also higher in CAS ($183 \mu\text{mol m}^{-2} \text{sec}^{-1}$) than AS ($157 \mu\text{mol m}^{-2} \text{sec}^{-1}$) plants, and in O ($181 \mu\text{mol m}^{-2} \text{sec}^{-1}$) than CO ($160 \mu\text{mol m}^{-2} \text{sec}^{-1}$) plants.

On-line ¹³C and fluorescence-based estimations of g_m reflect instantaneous measurements, and were thus not representative of the complete plant life cycle. A continuous difference in g_m will be reflected in the carbon isotope composition of the leaf dry matter (Evans *et al.*, 1986). Significant differences were found among plant lines in $\delta^{13}\text{C}$ of dry matter of leaves that developed during the 2 weeks subsequent to the first tetracycline application (Table 3), with the lowest values (-29.91‰) in O and the highest (-28.44‰) in AS plants. These differences in $\delta^{13}\text{C}$ were not correlated with the C_i/C_a ratio, but rather with the C_c/C_i ratio.

Discussion

The involvement of aquaporins in the regulation of g_m has been inferred from indirect evidence, like: (i) the prediction

Table 2 Photosynthetic characteristics of the studied genotypes (as determined at light saturation, 25°C and 400 $\mu\text{mol mol}^{-1} \text{CO}_2$). Values are means \pm SE of 12 (A_N , g_s , A_N/g_s , F_V/F_M , g_m , $\delta^{13}\text{C}$), six [carbonic anhydrase (CA) activity, RuBP content, respiration rate] or four (Rubisco activity and amount) replicates from independent plants per genotype

	CAS	AS	CO	O
A_N ($\mu\text{mol CO}_2 \text{ m}^{-2} \text{ sec}^{-1}$)	19.7 \pm 0.7	17.2 \pm 0.9*	18.5 \pm 0.6	21.9 \pm 0.8*
g_s ($\text{mol H}_2\text{O m}^{-2} \text{ sec}^{-1}$)	0.241 \pm 0.013	0.201 \pm 0.019*	0.208 \pm 0.012	0.271 \pm 0.021*
A_N/g_s ($\mu\text{mol CO}_2 \text{ mol H}_2\text{O}^{-1}$)	83 \pm 3	89 \pm 5	92 \pm 5	86 \pm 4
C_i ($\mu\text{mol mol}^{-1}$)	240.6 \pm 5.0	234.4 \pm 8.8	228.6 \pm 8.6	240.8 \pm 10.0
C_c ($\mu\text{mol mol}^{-1}$)	151.8 \pm 6.4	138.3 \pm 7.7*	189.3 \pm 8.9	211.1 \pm 11.6*
F_V/F_M	0.834 \pm 0.001	0.826 \pm 0.001*	0.837 \pm 0.002	0.837 \pm 0.002
Total Rubisco activity ($\mu\text{mol CO}_2 \text{ m}^{-2} \text{ sec}^{-1}$)	70 \pm 5	75 \pm 4	83 \pm 10	73 \pm 3
Rubisco holoenzyme ($\mu\text{mol m}^{-2}$)	2.7 \pm 0.1	2.8 \pm 0.2	3.4 \pm 0.4	2.9 \pm 0.2
CA activity ($\times 10^3$) ($\mu\text{mol CO}_2 \text{ m}^{-2} \text{ sec}^{-1}$)	1062 \pm 188	1247 \pm 198	2112 \pm 130	1979 \pm 161
RuBP content ($\mu\text{mol m}^{-2}$)	133 \pm 17	121 \pm 12	85 \pm 16	70 \pm 5
Respiration rate ($\mu\text{mol O}_2 \text{ m}^{-2} \text{ sec}^{-1}$)	-0.6 \pm 0.1	-0.6 \pm 0.1	-0.7 \pm 0.1	-0.7 \pm 0.1
g_m (Terashima) ($\text{mol CO}_2 \text{ m}^{-2} \text{ sec}^{-1}$)	0.247 \pm 0.021	0.179 \pm 0.012*	0.328 \pm 0.020	0.409 \pm 0.045*
g_m (Harley) ($\text{mol CO}_2 \text{ m}^{-2} \text{ sec}^{-1}$)	0.212 \pm 0.007	0.152 \pm 0.005*	0.288 \pm 0.016	0.366 \pm 0.034*
$\delta^{13}\text{C}$ in leaf dry matter (‰)	-28.87 \pm 0.11	-28.44 \pm 0.12*	-29.26 \pm 0.09	-29.91 \pm 0.11*

*Statistically significant ($P < 0.05$) differences between CAS and AS or between CO and O.

	CAS	AS	CO	O
(a)				
A_N ($\mu\text{mol CO}_2 \text{ m}^{-2} \text{ sec}^{-1}$)	15.2 \pm 1.1	13.5 \pm 1.2*	13.9 \pm 1.3	16.2 \pm 0.6*
g_s ($\text{mol H}_2\text{O m}^{-2} \text{ sec}^{-1}$)	0.351 \pm 0.078	0.257 \pm 0.071*	0.341 \pm 0.078	0.523 \pm 0.083*
C_i ($\mu\text{mol mol}^{-1} \text{CO}_2$)	269 \pm 9	245 \pm 11	270 \pm 9	289 \pm 6*
C_i/C_a	0.68 \pm 0.02	0.61 \pm 0.03*	0.67 \pm 0.02	0.72 \pm 0.01*
$\Delta(\text{‰})$	18.0 \pm 0.5	14.2 \pm 2.0*	17.9 \pm 0.8	19.4 \pm 0.7*
g_m ($\text{mol CO}_2 \text{ m}^{-2} \text{ sec}^{-1}$)	0.339 \pm 0.041	0.231 \pm 0.049*	0.323 \pm 0.048	0.451 \pm 0.079*
(b)				
A_N ($\mu\text{mol CO}_2 \text{ m}^{-2} \text{ sec}^{-1}$)	16.8 \pm 0.5	15.3 \pm 0.7*	17.0 \pm 1.4	18.4 \pm 0.4*
g_s ($\text{mol H}_2\text{O m}^{-2} \text{ sec}^{-1}$)	0.40 \pm 0.05	0.24 \pm 0.02*	0.36 \pm 0.06	0.56 \pm 0.05*
C_i ($\mu\text{mol mol}^{-1} \text{CO}_2$)	242 \pm 7	223 \pm 9	233 \pm 8	251 \pm 6
C_i/C_a	0.64 \pm 0.02	0.56 \pm 0.01*	0.61 \pm 0.02	0.66 \pm 0.02
$\Delta(\text{‰})$	15.7 \pm 0.5	14.6 \pm 0.2*	15.4 \pm 0.6	17.6 \pm 0.5*
Slope g_m ($\text{mol CO}_2 \text{ m}^{-2} \text{ sec}^{-1}$)	0.21 \pm 0.02	0.15 \pm 0.01*	0.20 \pm 0.01	0.29 \pm 0.04*

*Statistically significant ($P < 0.05$) differences between CAS and AS or between CO and O.^a g_m determined using on-line ^{13}C discrimination measurements with a dual-inlet mass spectrometer. Measurements were done at 400 $\mu\text{mol mol}^{-1} \text{CO}_2$, 1500 $\mu\text{mol photon m}^{-2} \text{ sec}^{-1}$, and 25°C. Values are means \pm SE of six replicates from independent plants per genotype.^b g_m determined using on-line discrimination with tunable diode laser absorption spectroscopy. Measurements are reported for 380 $\mu\text{mol mol}^{-1} \text{CO}_2$, 25°C, and saturating light except the slope-based g_m calculation which used light intensities from 400 to 2000 $\mu\text{mol photon m}^{-2} \text{ sec}^{-1}$. CO and O were not significantly different from each other for any parameter prior to tetracycline treatment (data not shown). Values are means \pm SE of three replicates from independent plants for CO, four for O and five for AS and CAS.

of a protein-facilitated diffusion process based on the temperature response of g_m (Bernacchi *et al.*, 2002), (ii) a decrease in g_m after exogenous application of HgCl_2 , a non-specific inhibitor of several aquaporins (Terashima and Ono, 2002), and (iii) evidence that the tobacco aquaporin NtAQP1 facilitates CO_2 membrane transport when inserted in *Xenopus* oocytes (Uehlein *et al.*, 2003). Our results clearly support a role for the aquaporin NtAQP1 in the regulation of g_m *in vivo*, under normal photosynthetic conditions.

In the present study we demonstrated that variation of NtAQP1 expression caused significant differences in g_m . Differences between CAS and AS or between CO and O were not accompanied by any considerable change in any of the morphological (Table 1) or physiological (Table 2) traits analysed. Only A_N and g_s , in addition to g_m , differed substantially among lines. Because these three parameters are usually co-regulated (Evans *et al.*, 1994; Flexas *et al.*, 2004), it is possible – but unlikely – that altering the

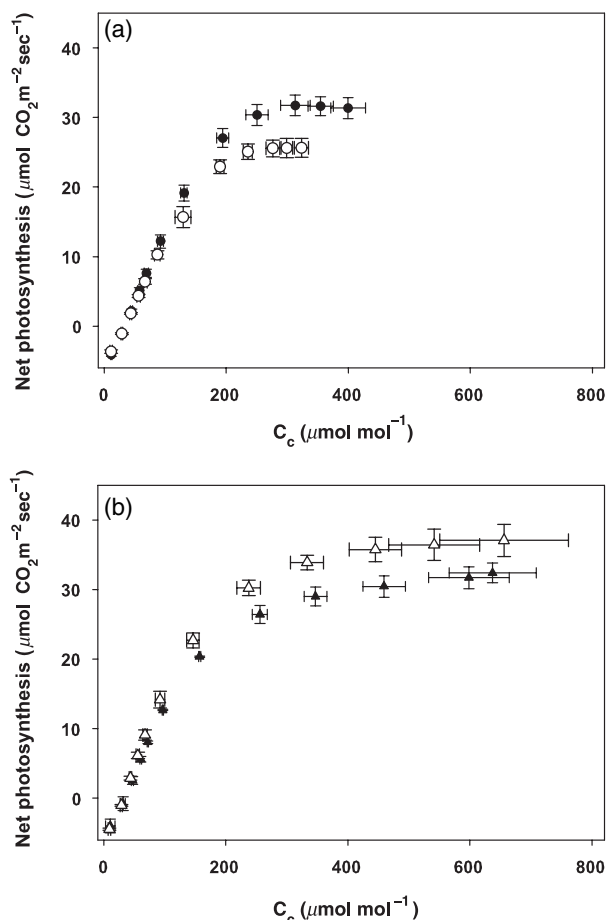


Figure 5. The response of net photosynthesis (A_N) to chloroplast CO₂ concentration (C_c) in CAS and AS (a) and CO and O (b). Values are means \pm SE of six replicates from independent plants per genotype. Symbols as in Figure 2.

expression of NtAQP1 resulted in a direct effect on A_N or g_s , and that g_m subsequently adjusted to these changes. The fact that NtAQP1 has been demonstrated to change CO₂ permeability of biological membranes (Uehlein *et al.*, 2003) strongly suggests that changing the amounts of NtAQP1 resulted in modified g_m . This, in turn, means an induced adjustment of A_N and g_s .

Alteration of g_m by changing NtAQP1 content without substantially modifying any other leaf trait analysed is in contrast with the results by Hanba *et al.* (2004). They found that transgenic rice plants overexpressing barley aquaporin HvPIP2;1 not only produced differences in g_m , but also in important anatomical (S_m , S_c , mesophyll porosity, stomatal density, stomatal size) and physiological (level of Rubisco) differences. This discrepancy could arise from the fact that in the study by Hanba *et al.* (2004) a foreign protein was expressed in transgenic plants while in the present study the levels of a native protein were modified. It is also evident that HvPIP2;1 and NtAQP1 belong to different aquaporin

subfamilies, i.e. PIP2 and PIP1, respectively, which show functional differences. In addition, rice and tobacco may have a different sensitivity of their acclimation responses. Despite these differences between the two studies, both suggest an important role for aquaporins in the regulation of g_m .

The involvement of aquaporins in the regulation of g_m provides a physiological basis for the observation that the response of g_m to drought, salinity or varying CO₂ concentration can be as strong and rapid as that of g_s (Centritto *et al.*, 2003; Flexas *et al.*, 2002, 2004). Although the mechanisms that regulate aquaporin activity in the short term are not fully understood, several mechanisms have been proposed, including direct phosphorylation of aquaporins (Kjellbom *et al.*, 1999), an osmotically driven cohesion/tension mechanism (Ye *et al.*, 2004), pH-dependent gating of aquaporins (Tournaire-Roux *et al.*, 2003) and transcriptional regulation and protein stability (Eckert *et al.*, 1999). Rapid regulation of g_m in response to environmental stresses may be an important mechanism for the observed photosynthetic downregulation.

Indeed, the 20–50% increase in g_m in O plants compared with CO plants was accompanied by a 15–20% increase in A_N at saturating light, depending on the experiment, which agrees with the observations of Aharon *et al.* (2003) and Hanba *et al.* (2004), who compared plants overexpressing Arabidopsis aquaporin PIP1;2 in transgenic tobacco and barley aquaporin HvPIP2;1 in rice, respectively. Therefore, the present results show that modifying the expression of a native aquaporin results in changes in g_m and photosynthesis. Not only did overexpression increase g_m and A_N , but it also reduced the expression of NtAQP1 in AS plants, resulting in a 20–40% decrease in g_m compared with CAS, and a 10–15% decrease in A_N . In contrast to saturating light conditions, at low light non-significant differences in A_N were found among genotypes (Figure 2). Most likely, this effect may be due to the fact that at subsaturating light photosynthesis is limited by electron transport and not by the availability of CO₂.

In addition to a modified g_m , different NtAQP1 levels resulted in light-saturated and CO₂-saturated photosynthesis, i.e. photosynthetic capacity (J_{max}) that differed by about 12% between CAS and AS and between CO and O. Also V_{cmax} was about 14% higher in O than in CO plants, but no differences were observed between AS and CAS plants. These results were unexpected, since photosynthetic capacity is not related to CO₂ diffusion but rather to the capacity of the photochemical and biochemical (Calvin cycle) machinery (Long and Bernacchi, 2003). This difference was clearly associated with NtAQP1 expression, since the differences between CO and O plants did not appear prior to the application of tetracycline (see Figure 4). We do not know at present the reason for such co-regulation

between g_m and the photosynthetic capacity. However, because altered g_m modified CO_2 concentrations in the chloroplast (and, presumably, the cytosol; Table 2), and CO_2 is a well-known regulator of the expression of several photosynthetic genes (Deng *et al.*, 2003; Ludewig and Sonnewald, 2000; Van Oosten *et al.*, 1994), we hypothesize that modified intercellular CO_2 concentrations trigger differences in the development of leaf photosynthetic capacity. This would also explain why g_m usually scales with photosynthetic capacity, as observed by broad comparisons between different species (Evans and Loreto, 2000; Evans *et al.*, 1994).

Finally, carbon isotope discrimination models (Evans *et al.*, 1986; Farquhar *et al.*, 1982) include a term for g_m that is often neglected. These models assume that most of the leaf discrimination against ^{13}C is due to discrimination by Rubisco and phosphoenolpyruvate carboxylase, with another minor fractionation due to CO_2 diffusion in air through stomata. As a result, ^{13}C discrimination (Δ) is proportional to the C_i/C_a ratio, and $\delta^{13}\text{C}$ in leaf dry matter is interpreted as resulting from the 'mean leaf-life' C_i/C_a ratio, which can be related to intrinsic efficiency of water use (A_N/g_s). Therefore, $\delta^{13}\text{C}$ in leaf dry matter has been used as a long-term estimation to compare efficiency of water use between species or genotypes. The present results demonstrate that discrimination during CO_2 diffusion within the leaf should not be neglected. Substantial differences were found in leaf $\delta^{13}\text{C}$ between different lines with only small changes in their C_i/C_a ratio, which weakens the correlation between $\delta^{13}\text{C}$ and efficiency of water use. However, differences in $\delta^{13}\text{C}$ were strongly correlated with C_i/C_a ratio and g_m (not shown) as suggested by Le Roux *et al.* (2001). These experimental data match well with theoretical calculations by Warren and Adams (2006) that showed that differences in g_m could induce a difference of up to 2–4‰ in leaf $\delta^{13}\text{C}$ without any difference in the efficiency of water use.

In summary, the present results provide evidence that NtAQP1 is involved in g_m regulation *in vivo*. They also strengthen the need to incorporate a term that considers g_m in current photosynthesis models, such as that by Farquhar *et al.* (1980), as already suggested by Bernacchi *et al.* (2002) and Ethier and Livingston (2004). Clearly, the response of A_N to C_i significantly differed between lines (Figure 3). According to the Farquhar *et al.* model, this may be interpreted in terms of differences in the maximum carboxylation rate (V_{cmax}) and the maximum electron transport rate (J_{max}). However, once g_m is used to assess the response of A_N to C_c the results are rather different, showing that V_{cmax} does not differ (CAS versus AS) or differs to a lesser extent (CO versus O), but J_{max} still differs substantially among genotypes. Therefore, including a g_m term would improve the predictive accuracy of the photosynthesis models.

Experimental procedures

Plant material

Antisense and overexpressing tobacco plants (*Nicotiana tabacum* L.) were obtained from different lines: var. Samsun for the antisense (AS) lines (Siefritz *et al.*, 2002) and line Hö 20.20 for the overexpressing (O) lines (Uehlein *et al.*, 2003). Plants of each line with normal NtAQP1 expression were used as controls (CAS and CO).

For initial characterization, three independently transformed antisense lines were selected. Plants from individual lines were self-fertilized and the T_4 was subjected to further analysis. Each line was transformed with a single NtAQP1 antisense construct, as confirmed by Southern hybridization, and showed a reduction of NtAQP1 expression of between 90% and 95% at the mRNA level. The three lines were chosen for data assessments and the data for all measurements were pooled. For characterization of NtAQP1 overexpressing lines three independently transformed lines were initially characterized. All showed an increase in NtAQP1 expression after treatment with tetracycline. A representative line was chosen for further experiments.

In AS lines NtAQP1 expression was inhibited by a 35SCaMV promoter-driven antisense construct, while in O lines the NtAQP1 coding region was under the control of a tetracycline-inducible promoter (Uehlein *et al.*, 2003). For the initial experiment, six to eight plants per line were germinated and grown in a growth chamber in 5-l pots containing a mixture of perlite, horticultural substrate and clay. The environmental conditions were set to a 12-h photoperiod (25°C day/20°C night), 40–60% relative humidity and a photon flux density at plant height of about 800–1000 $\mu\text{mol m}^{-2} \text{sec}^{-1}$ (halogen lamps). Plants were irrigated daily at pot capacity with 100% Hoagland's solution during the entire experiment. All plants were 7 weeks old at the beginning and 14 weeks old at the end of the experiments.

For induction of NtAQP1 expression in O plants, pots were watered with 10 mg l^{-1} tetracycline once a day, and photosynthetic measurements were performed 2 or 3 days after tetracycline treatment. The CO plants were also irrigated with tetracycline to compensate for any possible indirect effect of tetracycline besides NtAQP1 expression. These plants continued being irrigated with tetracycline until the end of the experiments, about 3 weeks later, and they developed between three and six new leaves during that time. These most recently developed leaves were sampled for carbon isotope analysis at the end of the experiment.

Two additional experiments were performed using the same four lines described to confirm the results, one at the Universitat de les Illes Balears, Spain (UIB) and one jointly at the University of New Mexico (UNM) and the Los Alamos National Laboratory (LANL), USA. At UIB, seeds were germinated in early August, and the plants were grown under ambient conditions during autumn in a greenhouse in 10-l pots containing a mixture of perlite, horticultural substrate and clay. Plants were irrigated daily at pot capacity with 50% Hoagland's solution during the entire experiment, and were 14 weeks old when measured. At UNM, seeds were germinated in late September and plants were grown under greenhouse conditions (25/20°C day/night) for 6 weeks and then transported to a greenhouse in LANL. Plants were allowed to acclimate to the new conditions (25/16°C day/night) for at least 2 weeks prior to measurement with supplementary light to maintain a 14-h photoperiod. Plants were grown in 10-l pots containing a commercial soil-less peat mix (Metro-mix 360, W.R. Grace and Company, Cambridge, MA, USA), watered daily to field capacity with a half-strength commercial fertilizer (Jack's 20-20-20, J.R. Peters, Inc., Allentown, PA, USA) and supplemented every 2 weeks (0.15 ml l^{-1}) with a

commercial micronutrient mix (Micrel Total 5-0-0, Growth Products, Ltd, White Plains, NY, USA). To induce overexpression in O plants, application of tetracycline was as described for the previous experiment and measurements were conducted 4–6 days after initiation of treatment.

Plant water status, leaf mass area and plant size determinations

The leaf relative water content (RWC) was determined as follows: $RWC = (\text{fresh weight} - \text{dry weight}) / (\text{turgid weight} - \text{dry weight})$. To determine the turgid weight, leaves were kept in distilled water in darkness at 4°C to minimize respiration losses until they reached a constant weight (full turgor, typically after 12 h). Their dry weight was obtained after 48 h at 70°C in an oven. Leaf mass area (LMA) was calculated from leaf dry weight and leaf area as $LMA = \text{dry weight} / \text{leaf area}$.

Plant height, basal stem diameter, leaf length and total number of leaves per plant were measured at the end of the experiments. Plant height, leaf length and basal shoot diameter were also measured.

Light microscopy and leaf mesophyll traits

Small pieces of leaf (2 mm²) were sampled after gas exchange measurements and fixed in 2.5% glutaraldehyde in 25 mM sodium cacodylate buffer (pH 7.2) at 4°C for 2 days. The samples were post-fixed in 2% osmium tetroxide for 3–5 h, dehydrated in acetone and propylene series, and embedded in Spurr's resin. For light microscopy, sections were cut at 0.8 μm thick with an ultramicrotome and stained with toluidine blue. Sections were photographed at magnification of 100× and 500× (Miyazawa and Terashima, 2001). The photographs were quantitatively analysed using the ArcView 3.2 GIS software package (ESRI, Redlands, CA, USA). Following Syversten *et al.* (1995), the areas of mesophyll (S_m) and chloroplast (S_c) surfaces directly exposed to the intercellular air spaces on a leaf area basis were determined. Cells were assumed to be cylindrical, and a curvature factor of 1.36 was applied after Syversten *et al.* (1995).

Carbon isotope composition in leaf dry matter

At the end of the experiments, the most recently developed leaves were sampled from each line, dried for 48 h at 70°C, ground into powder and subsampled for analysis of the C isotope ratios. Samples were combusted in an elemental analyser (Carlo-Erba, Rodano, Italy), CO₂ was separated by chromatography and directly injected into a continuous-flow isotope ratio mass spectrometer (Thermo Finnigan Delta Plus, Bremen, Germany). Peach leaf (NIST 1547) standards were run every six samples. The standard deviation of the analysis was below 0.1‰. The calculation of the isotope ratio ($\delta^{13}\text{C}$) was done as $\delta^{13}\text{C}_{\text{sample}}(\text{‰}) = (R_{\text{sample}}/R_{\text{standard}} - 1) \times 1000$ (Farquhar *et al.*, 1982), where $R_{\text{sample}}/R_{\text{standard}}$ were referred to a Pee Dee Belemnite standard.

Dark respiration rates

Dark respiration rates were determined at 25°C in leaf discs using a liquid-phase O₂ electrode (OXY042A, Rank Brothers, Cambridge, UK), to avoid any possible interference of the CO₂ released with the partial pressure of oxygen in a closed cuvette (Davey *et al.*, 2004).

Enzyme activities and metabolite contents

For measurements of RuBP content, six discs (5.3 cm²) per line of fully illuminated leaves at ambient CO₂ were freeze clamped into liquid nitrogen and stored at –70°C until assay. Extraction and assays were performed following Giménez *et al.* (1992).

Assays of Rubisco activity were performed on leaf punches (1.56 cm²) that were immediately frozen in liquid N₂ after gas exchange measurements and stored at –70°C until analysis. Extraction and assay of total Rubisco activity was performed as in Whitney *et al.* (1999) and Sharkey *et al.* (1991) respectively. Total Rubisco content was also determined from activated aliquots via stoichiometric binding of ¹⁴C-carboxyarabinitol bisphosphate (¹⁴CABP) and gel filtration (Butz and Sharkey, 1989; Ruuska *et al.*, 1998).

Measurements of carbonic anhydrase activity were performed following the method of Gillon and Yakir (2000).

Measurements of gas exchange and chlorophyll fluorescence

Leaf gas exchange was determined simultaneously with measurements of chlorophyll fluorescence using the open gas exchange system Li-6400 (Li-Cor Inc., Lincoln, NE, USA) with an integrated fluorescence chamber head (Li-6400-40; Li-Cor Inc.). Measurements were made on the youngest fully expanded leaf before stem elongation. In dark-adapted leaves (i.e. pre-dawn), the maximum photochemical efficiency of photosystem II (F_v/F_m) was determined as $F_v/F_m = (F_m - F_0)/F_m$ by measuring basal fluorescence (F_0) and maximum fluorescence during a light-saturating pulse of about 8000 μmol m⁻² sec⁻¹ (F_m). In light-adapted leaves, the actual photochemical efficiency of photosystem II (ϕ_{PSII}) was determined by measuring steady-state fluorescence (F_s) and maximum fluorescence (F'_m) during a light-saturating pulse of about 8000 μmol m⁻² sec⁻¹ (ϕ_{PSII}) following Genty *et al.* (1989):

$$\phi_{\text{PSII}} = (F'_m - F_s)/F'_m$$

The electron transport rate (J) was then calculated as:

$$J = \phi_{\text{PSII}} \times \text{PFD} \times \alpha$$

where PFD is the photosynthetically active photon flux density and α is a term which includes the product of leaf absorption and the partitioning of absorbed quanta between photosystems I and II. α was previously determined for each line as the slope of the relationship between ϕ_{PSII} and ϕ_{CO_2} obtained by varying light intensity under non-photorespiratory conditions in an atmosphere containing <1% O₂ (Valentini *et al.*, 1995). These two relationships passed through the origin. α was 0.408 for CAS and AS plants and 0.364 for CO and O plants.

In light-adapted leaves, photosynthesis was induced in saturating light (1000 μmol m⁻² sec⁻¹) and 400 μmol mol⁻¹ CO₂ surrounding the leaf (C_a). The amount of blue light was set to 15% PFD to optimize stomatal aperture. Leaf temperature was maintained at 25°C, and the leaf-to-air vapour pressure deficit was kept between 1 and 2 kPa during all measurements. Once steady state was reached (usually between 30 and 60 min after clamping the leaf), either a light-response curve or a CO₂-response curve was measured. Six light-response curves and six CO₂-response curves were obtained for each plant line. Leakage of CO₂ into and out of the empty chamber was determined for the range of CO₂ concentrations used in this study and used to correct measured leaf fluxes (Bernacchi *et al.*, 2002; Long and Bernacchi, 2003).

Estimation of g_m by gas exchange and chlorophyll fluorescence

Two different methods using simultaneous gas exchange and chlorophyll fluorescence measurements were used to estimate g_m , as described by Terashima and Ono (2002) and Harley *et al.* (1992), respectively.

The method of Terashima and Ono (2002) consists of a comparison of the initial slopes of the A_N-C_i and the A_N-C_c curves. C_i was calculated with the usual gas exchange procedures (Long and Bernacchi, 2003). C_c was estimated according to procedures described by Epron *et al.* (1995) as:

$$C_c = (O/S)\{[J + 8(A_N + R_l)]/(2J) - 8(A_N + R_l)\}$$

where O is the O_2 concentration in the chloroplast (assumed to be $0.21 \text{ mol mol}^{-1}$), S is the specificity factor of Rubisco and R_l is the rate of mitochondrial respiration in the light. The value of S was considered to be $2459 \text{ mol mol}^{-1}$, corresponding to a CO_2 compensation point in the absence of respiration (Γ^*) of $42.75 \text{ } \mu\text{mol mol}^{-1}$ (Bernacchi *et al.*, 2002). R_l was calculated using a linear regression line of the relationship between A_N and C_i for the range of C_i below $150 \text{ } \mu\text{mol mol}^{-1}$. A_N at Γ^* was assumed to be equal to $-R_l$ (Brooks and Farquhar, 1985). g_m was obtained as:

$$g_m = (m_i m_c)/(m_c - m_i)$$

where m_i and m_c are the slopes of the A_N-C_i and the A_N-C_c curves, respectively, at C_i below $200 \text{ } \mu\text{mol mol}^{-1}$ and C_c below $150 \text{ } \mu\text{mol mol}^{-1}$.

The method by Harley *et al.* (1992) uses A_N and R_l measured from gas exchange and J estimated from fluorescence to calculate g_m as follows:

$$g_m = A_N / (C_i - \{\Gamma^* [J + 8(A_N + R_l)] / [J - 4(A_N + R_l)]\})$$

Γ^* and R_l were estimated as in the previous method. For the Harley method, estimations of g_m were done at $C_a = 400 \text{ } \mu\text{mol mol}^{-1}$.

The primary difference between the two methods is that the first integrates a g_m value for the whole CO_2 -limited region of the CO_2 -response curve, while the second estimates a g_m value for each separate point of the curve.

Estimation of g_m by carbon isotope discrimination

Two additional methods based on ^{13}C discrimination were used for estimations of g_m in additional experiments, one at the UIB and one jointly at the UNM and LANL.

At UIB, gas exchange parameters were measured as described with a LI-6400 system under steady-state conditions for a minimum of 45 min. For instantaneous carbon isotope discrimination, the air exiting the cuvette through the match valve system was passed through a magnesium perchlorate water trap and collected in a hand-made 100 ml glass flask at a flow rate of 150 ml min^{-1} . Once the steady state was reached, the stopcocks of the flasks were closed. Two sets of flasks were collected, one in the presence of the leaf (sample) and one in the absence of the leaf (reference). CO_2 from the collected air was concentrated in a sample loop under liquid nitrogen and introduced to the corresponding dual-inlet bellow. Carbon isotope discrimination was measured in a dual-inlet isotope ratio mass spectrometer (Thermo, Delta XPlus, Bremen, Germany). The dual-inlet analysis of the isotope ratio compared the CO_2 from the sample gas with the CO_2 from the reference gas. Carbon isotope discrimination was calculated as described by Evans *et al.* (1986), as:

$$\Delta^{13}C_{obs} = \xi(\delta^{13}C_o - \delta^{13}C_e) / [1000 + \delta^{13}C_o - \xi(\delta^{13}C_o - \delta^{13}C_e)]$$

where $\xi = C_e/(C_e - C_o)$, and C_e and C_o are the CO_2 concentrations entering and leaving the gas-exchange cuvette, respectively. Gas-exchange parameters A_N , C_e and C_o , were as determined with the LI-6400, and $\delta^{13}C_e$ equalled 0 and $\delta^{13}C_o$ was the measured discrimination value. Mesophyll conductance was determined by comparison of the expected discrimination, where C_i is equal to C_c , and the measured discrimination, as described by Evans *et al.* (1986).

At UNM, gas exchange parameters were measured using a LI-6400 system in conjunction with a tuneable diode laser absorbance spectrometer (TDLAS) (TGA100A, Campbell Scientific, Logan, UT, USA) which measures absolute concentrations of $^{13}CO_2$ and $^{12}CO_2$ in air (Bowling *et al.*, 2003). The TDLAS was adapted from atmospheric sampling to leaf-level measurement of on-line, real-time carbon isotope discrimination by subsampling air entering the LI-6400 reference IRGA and the air leaving the leaf cuvette through the match valve port (DTH, unpublished). Both air streams were dried with a Nafion dryer prior to analysis (PD625 dual configuration, Campbell Scientific, Logan, UT, USA). The TDLAS samples at an approximate flow rate of 190 ml min^{-1} and LI-6400 flows were maintained slightly above this to ensure the room air was not sampled. A 'T' junction with one side open to the room was placed between the LI-6400 and the TDLAS to avoid pressure changes related to TDLAS subsampling. The empty, closed leaf cuvette was also measured before and after each leaf to correct for slight variation caused by changes in gasket leakiness between samples.

Upon clamping each leaf in the cuvette leaves were exposed to $2000 \text{ } \mu\text{mol photons m}^{-2} \text{ sec}^{-1}$ light, $380 \text{ } \mu\text{mol } CO_2 \text{ mol}^{-1}$ air, flow of $220 \text{ } \mu\text{mol sec}^{-1}$, and relative humidity around 50%. When steady-state was achieved the leaf was sampled for another 6 min (three 2-min cycles). The light intensity was decreased stepwise to $400 \text{ } \mu\text{mol photons m}^{-2} \text{ sec}^{-1}$ and measurements were continued for at least 6 min after steady state at each light intensity.

Carbon isotope discrimination was calculated according to Evans *et al.* (1986) as described above. Mesophyll conductance values were determined by comparing predicted discrimination (Δ_i) with $\Delta^{13}C_{obs}$ across the entire light-response curve using the slope of ($\Delta_i - \Delta^{13}C_{obs}$)/ p_i/p_a versus A_N/p_i where p_i and p_a are the intercellular and ambient partial pressures of CO_2 respectively (Equation 5 in von Caemmerer and Evans, 1991).

Protein extraction, separation and Western blotting

At the end of the experiments, fresh leaf material (50–100 mg per sample) was collected from several plants of each genotype, and ground in 1 ml buffer containing 5 mM EDTA, 5 mM EGTA, 10 mM KPO_4 pH 7.8 supplemented with Protease-Inhibitors from Sigma (St. Louis, MO, USA), followed by a 5-min centrifugation at 800 g in a tabletop-centrifuge. The supernatant was transferred to a new tube and mixed with a 4× concentrated Laemmli buffer (100 mM Tris pH 6.8, 200 mM DTT, 40% glycerol, 4% SDS, 0.2% bromphenol blue). Equal amounts (5 μg) of protein per lane were loaded on a PAGE gel and run at 30 mA.

Western blotting was then performed as described by Santoni *et al.* (2003), with some modifications. Proteins were transferred to Protran B83 (Whatman, Middlesex, UK) in 10% methanol, 10 mM 3-(cyclohexylamino)-1-propanesulfonic acid (CAPS), pH 11 for 16 h at 35 V. The membrane was blocked for 1 h in phosphate-buffered saline containing 0.1% (v.v) Tween 20 and 1% BSA and subsequently incubated with the primary antibody (1:5000 dilution) for 2 h at room temperature. After washing ($2 \times 10 \text{ min}$) in the phosphate buffer described above, the blot was incubated for 1 h

with a phosphatase-labelled secondary antibody. After washing (2× 10 min) in phosphate-buffered saline, a chemiluminescent signal using CDP Star (Applied Biosystems, Foster City, CA, USA) substrate was visualized on an autoradiography film (Hyperfilm, GE Healthcare, Amersham Biosciences, Piscataway, NJ, USA).

Statistical analysis

One-way ANOVA was applied to assess the differences for each parameter between each separate control and its derivative line. Differences among means were established using a Duncan test ($P < 0.05$). The data were analysed applying the spss 10.0 programme for Windows. At UNM comparisons between control and derivative lines were analysed using pairwise *t*-tests calculated with Microsoft Excel 2002.

Acknowledgements

This work was supported by CICYT Projects BFI2002-00772 and BFU2005-03102/BFI (Plan Nacional, Spain) and DFG Project Ka 1032/15-1 to R.K. (Deutsche Forschungsgemeinschaft). MR-C was the beneficiary of a contract from Programa Ramón y Cajal (M.E.C.). Financial support to JB from Beca d'Investigació UIB is appreciated. Research conducted in New Mexico was supported by IGPP project 095566-001-05 (LANL, USA) and RAC projects 04-38 and 05-L-07 (UNM, USA). We thank Drs J.A. Berry, F. Loreto and I. Terashima for constructive and insightful comments on data and methodology. We would like to thank Drs Regina Galarza and Pedro Aparicio-Tejo at the Universidad Pública de Navarra and Dr Biel Martorell from Serveis Científicotècnics, UIB for their technical assistance and availability of their gas chromatograph-isotope ratio mass spectrometer. Dr Ferran Hierro and Mrs Maria Pocoví, from Serveis Científicotècnics, UIB, and Ms Jerònia Ramon, from Servei de Sistemes d'Informació Geogràfica i Teledetecció, UIB, helped with microscopy and image analysis, respectively. Karen Brown, LANL, also assisted with TDL-based measurements of mesophyll conductance.

References

- Aharon, R., Shalak, Y., Winiger, S., Bendov, R. and Kapulnik, Y. (2003) Overexpression of a plasma membrane aquaporin in transgenic tobacco improves plant vigor under favourable growth conditions but not under drought or salt stress. *Plant Cell*, **15**, 439–447.
- Baiges, I., Schäffner, A.R., Affenzeller, M.J. and Mas, A. (2002) Plant aquaporins. *Physiol. Plant*, **115**, 175–182.
- Beitz, E., Wu, B.H., Holm, L.M., Schultz, J.E. and Zeuthen, T. (2006) Point mutations in the aromatic/arginine region in aquaporin 1 allow passage of urea, glycerol, ammonia, and protons. *Proc. Natl Acad. Sci. USA*, **103**, 269–274.
- Bernacchi, C.J., Portis, A.R., Nakano, H., von Caemmerer, S. and Long, S.P. (2002) Temperature response of mesophyll conductance. Implications for the determination of Rubisco enzyme kinetics and for limitations to photosynthesis *in vivo*. *Plant Physiol.* **130**, 1992–1998.
- Biela, A., Grote, K., Otto, B., Hedrich, R. and Kaldenhoff, R. (1999) The *Nicotiana tabacum* plasma membrane aquaporin NTAQP1 is mercury-insensitive and permeable for glycerol. *Plant J.* **18**, 565–570.
- Bongi, G. and Loreto, F. (1989) Gas-exchange properties of salt-stressed olive (*Olea europaea* L.) leaves. *Plant Physiol.* **90**, 1408–1416.
- Bowling, D.R., Sargent, S.D., Tanner, B.D. and Ehleringer, J.R. (2003) Tunable diode laser absorption spectroscopy for stable isotope studies of ecosystem-atmosphere CO₂ exchange. *Agric. For. Meteorol.* **118**, 1–19.
- Brooks, A. and Farquhar, G.D. (1985) Effect of temperature on the CO₂/O₂ specificity of ribulose-1,5-bisphosphate carboxylase/oxygenase and the rate of respiration in the light. *Planta*, **165**, 397–406.
- Brugnoli, E., Scartazza, A., Lauteri, M., Monteverdi, M.C. and Máguas, C. (1998) Carbon isotope discrimination in structural and non-structural carbohydrates in relation to productivity and adaptation to unfavourable conditions. In *Stable Isotopes. Integration of Biological, Ecological and Geochemical Processes* (Griffiths, H. ed). Oxford: BIOS Scientific Publishers, pp. 133–144.
- Butz, N.D. and Sharkey, T.D. (1989) Activity ratios of ribulose-1,5-bisphosphate carboxylase accurately reflect carbamylation ratios. *Plant Physiol.* **89**, 735–739.
- von Caemmerer, S. and Evans, J.R. (1991) Determination of the average partial pressure of CO₂ in chloroplasts from leaves of several C₃ plants. *Aust. J. Plant Physiol.* **18**, 287–305.
- Centritto, M., Loreto, F. and Chartzoulakis, K. (2003) The use of low [CO₂] to estimate diffusional and non-diffusional limitations of photosynthetic capacity of salt-stressed olive saplings. *Plant Cell Environ.* **26**, 585–594.
- Chrispeels, M.J., Morillon, R., Maurel, C., Gerbeau, P., Kjellbom, P. and Johansson, I. (2001) Aquaporins in plants: structure, function, regulation and roles in plant water relations. *Curr. Top. Membr.* **51**, 277–334.
- Cooper, G.J. and Boron, W.F. (1998) Effect of PCMBs on CO₂ permeability on *Xenopus* oocytes expressing aquaporin 1 or its C189S mutant. *Am. J. Physiol. Cell Physiol.* **44**, C1481–C1486.
- Davey, P.A., Hunt, S., Hymus, G.J., De Lucia, E.H., Drake, B.G., Karnosky, D.F., Long, S.P. (2004) Respiratory oxygen uptake is not decreased by an instantaneous elevation of [CO₂], but is increased with long-term growth in the field at elevated [CO₂]. *Plant Physiol.* **134**, 520–527.
- Delfine, S., Alvino, A., Zacchini, M. and Loreto, F. (1998) Consequences of salt stress on conductance to CO₂ diffusion, Rubisco characteristics and anatomy of spinach leaves. *Aust. J. Plant Physiol.* **25**, 395–402.
- Delfine, S., Alvino, A., Villani, M.C. and Loreto, F. (1999) Restrictions to carbon dioxide conductance and photosynthesis in spinach leaves recovering from salt stress. *Plant Physiol.* **119**, 1101–1106.
- Deng, Y., Ye, J. and Mi, H. (2003) Effects of Low CO₂ on NAD(P)H dehydrogenase, a mediator of cyclic electron transport around photosystem I in the cyanobacterium *Synechocystis* PCC6803. *Plant Cell Physiol.* **44**, 534–540.
- Di Marco, G., Manes, F., Tricoli, D. and Vitale, E. (1990) Fluorescence parameters measured concurrently with net photosynthesis to investigate chloroplastic CO₂ concentration in leaves of *Quercus ilex* L. *J. Plant Physiol.* **136**, 538–543.
- Düring, H. (2003) Stomatal and mesophyll conductances control CO₂ transfer to chloroplasts in leaves of grapevine (*Vitis vinifera* L.). *Vitis*, **42**, 65–68.
- Eckert, M., Biela, A., Siefert, F., Kaldenhoff, R. (1999) New aspects of plant aquaporin regulation and specificity. *J. Exp. Bot.* **50**, 1541–1545.
- Epron, D., Godard, D., Cornic, G. and Genty, B. (1995) Limitation of net CO₂ assimilation rate by internal resistances to CO₂ transfer in the leaves of two tree species (*Fagus sylvatica* L. and *Castanea sativa* Mill.). *Plant Cell Environ.* **18**, 43–51.
- Ethier, G.J. and Livingston, N.J. (2004) On the need to incorporate sensitivity to CO₂ transfer conductance into the Farquhar-von

- Caemmerer – berry leaf photosynthesis model. *Plant Cell Environ.* **27**, 137–153.
- Evans, J.R. and von Caemmerer, S.** (1996) Carbon dioxide diffusion inside leaves. *Plant Physiol.* **110**, 339–346.
- Evans, J.R. and Loreto, F.** (2000) Acquisition and diffusion of CO₂ in higher plant leaves. In *Photosynthesis: Physiology and Metabolism* (Leegood, R.C., Sharkey, T.D. and von Caemmerer, S., eds). The Netherlands: Kluwer Academic Publishers, pp. 321–351.
- Evans, J.R., Sharkey, T.D., Berry, J.A. and Farquhar, G.D.** (1986) Carbon isotope discrimination measured concurrently with gas exchange to investigate CO₂ diffusion in leaves of higher plants. *Aust. J. Plant Physiol.* **13**, 281–292.
- Evans, J.R., von Caemmerer, S., Setchell, B.A. and Hudson, G.S.** (1994) The relationship between CO₂ transfer conductance and leaf anatomy in transgenic tobacco with a reduced content of Rubisco. *Aust. J. Plant Physiol.* **21**, 475–495.
- Farquhar, G.D., von Caemmerer, S. and Berry, J.A.** (1980) A biochemical model of photosynthetic CO₂ assimilation in leaves of C₃ species. *Planta*, **149**, 78–90.
- Farquhar, G.D., O'Leary, M.H. and Berry, J.A.** (1982) On the relationship between carbon isotope discrimination and the intercellular carbon dioxide concentration in leaves. *Aust. J. Plant Physiol.* **9**, 121–137.
- Flexas, J., Bota, J., Escalona, J.M., Sampol, B. and Medrano, H.** (2002) Effects of drought on photosynthesis in grapevines under field conditions: an evaluation of stomatal and mesophyll limitations. *Funct. Plant Biol.* **29**, 461–471.
- Flexas, J., Bota, J., Loreto, F., Cornic, G. and Sharkey, T.D.** (2004) Diffusive and metabolic limitations to photosynthesis under drought and salinity in C₃ plants. *Plant Biol.* **3**, 269–279.
- Genty, B., Briantais, J.M. and Baker, N.R.** (1989) The relationship between the quantum yield of photosynthetic electron transport and quenching of chlorophyll fluorescence. *Biochim. Biophys. Acta*, **990**, 87–92.
- Gillon, J.S. and Yakir, D.** (2000) Internal conductance to CO₂ diffusion and C¹⁸O discrimination in C₃ leaves. *Plant Physiol.* **123**, 201–213.
- Giménez, C., Mitchell, V.J. and Lawlor, D.W.** (1992) Regulation of photosynthesis rate of two sunflower hybrids under water stress. *Plant Physiol.* **98**, 516–524.
- Hanba, Y.T., Miyazawa, S.-I., Kogami, H., Terashima, I.** (2001) Effects of leaf age on internal CO₂ transfer conductance and photosynthesis in tree species having different types of shoot phenology. *Aust. J. Plant Physiol.* **28**, 1075–1084.
- Hanba, Y.T., Shibasaka, M., Hayashi, Y., Hayakawa, T., Kasamo, K., Terashima, I. and Katsuhara, M.** (2004) Overexpression of the barley aquaporin HvPIP2;1 increases internal CO₂ conductance and CO₂ assimilation in the leaves of transgenic rice plants. *Plant Cell Physiol.* **45**, 521–529.
- Harley, P.C. and Sharkey, T.D.** (1991) An improved model of C₃ photosynthesis at high CO₂: reversed O₂ sensitivity explained by lack of glycerate reentry into the chloroplast. *Photosynth. Res.* **27**, 169–178.
- Harley, P.C., Loreto, F., Di Marco, G. and Sharkey, T.D.** (1992) Theoretical considerations when estimating the mesophyll conductance to CO₂ flux by analysis of the response of photosynthesis to CO₂. *Plant Physiol.* **98**, 1429–1436.
- Holm, L.M., Klaerke, D.A. and Zeuthen, T.** (2004) Aquaporin 6 is permeable to glycerol and urea. *Pflug. Arch. Eur. J. Phy.* **448**, 181–186.
- Jahn, T.P., Moller, A.L.B., Zeuthen, T., Holm, L.M., Klaerke, D.A., Mohsin, B., Kuhlbrandt, W. and Schjoerring, J.K.** (2004) Aquaporin homologues in plants and mammals transport ammonia. *FEBS Lett.* **574**, 31–36.
- Kaldenhoff, R., Grote, K., Zhu, J.J. and Zimmermann, U.** (1998) Significance of plasmalemma aquaporins for water-transport in *Arabidopsis thaliana*. *Plant J.* **14**, 121–128.
- Kjellbom, P., Larsson, C., Johanson, I., Karlsson, M. and Johanson, U.** (1999) Aquaporins and water homeostasis in plants. *Trends Plant Sci.* **4**, 308–314.
- Le Roux, X., Bariac, T., Sinoquet, H., Genty, B., Piel, C., Mariotti, A., Girardin, C. and Richard, P.** (2001) Spatial distribution of leaf water-use efficiency and carbon isotope discrimination within an isolated tree crown. *Plant Cell Environ.* **24**, 1021–1032.
- Liu, L.H., Ludewig, U., Gassert, B., Frommer, W.B. and von Wiren, N.** (2003) Urea transport by nitrogen-regulated tonoplast intrinsic proteins in *Arabidopsis*. *Plant Physiol.* **133**, 1220–1228.
- Lloyd, J., Syvertsen, J.P., Kriedemann, P.E. and Farquhar, G.D.** (1992) Low conductances for CO₂ diffusion from stomata to the sites of carboxylation in leaves of woody species. *Plant Cell Environ.* **15**, 873–899.
- Long, S.P. and Bernacchi, C.J.** (2003) Gas exchange measurements, what can they tell us about the underlying limitations to photosynthesis? Procedures and sources of error. *J. Exp. Bot.* **54**, 2393–2401.
- Loreto, F., Harley, P.C., Di Marco, G. and Sharkey, T.D.** (1992) Estimation of mesophyll conductance to CO₂ flux by three different methods. *Plant Physiol.* **98**, 1437–1443.
- Loreto, F., Di Marco, G., Tricoli, D. and Sharkey, T.D.** (1994) Measurements of mesophyll conductance, photosynthetic electron transport and alternative electron sinks of field grown wheat leaves. *Photosynth. Res.* **41**, 397–403.
- Loreto, F., Centritto, M. and Chartzoulakis, K.** (2003) Photosynthetic limitations in olive cultivars with different sensitivity to salt stress. *Plant Cell Environ.* **26**, 595–601.
- Ludewig, F. and Sonnewald, U.** (2000) High CO₂-mediated down-regulation of photosynthetic gene transcripts is caused by accelerated leaf senescence rather than sugar accumulation. *FEBS Lett.* **11**, 19–24.
- Makino, A., Sakashita, H., Hidema, J., Mae, T., Ojima, K. and Osmond, B.** (1992) Distinctive responses of ribulose-1,5-bisphosphate carboxylase and carbonic anhydrase in wheat leaves to nitrogen nutrition and their possible relationship to CO₂ transfer resistance. *Plant Physiol.* **100**, 1737–1743.
- Manter, D.K. and Kerrigan, J.** (2004) A/C_i curve analysis across a range of woody plant species: influence of regression analysis parameters and mesophyll conductance. *J. Exp. Bot.* **55**, 2581–2588.
- Maurel, C. and Chrispeels, M.J.** (2001) Aquaporins. A molecular entry into plant water relations. *Plant Physiol.* **125**, 135–138.
- Maurel, C., Kado, R.T., Guern, J. and Chrispeels, M.J.** (1993) The vacuolar membrane protein d-TIP creates water specific channels in *Xenopus* oocytes. *EMBO J.* **12**, 2241–2247.
- Maurel, C., Tacnet, F., Güclü, J., Guern, J. and Ripoche, P.** (1997) Purified vesicles of tobacco cell vacuolar and plasma membranes exhibit dramatically different water permeability and water channel activity. *Proc. Natl Acad. Sci. USA*, **94**, 7103–7108.
- Meinild, A.K., Klaerke, D.A. and Zeuthen, T.** (1998) Bidirectional water fluxes and specificity for small hydrophilic molecules in aquaporins 0–5. *J. Biol. Chem.* **273**, 32446–32451.
- Miyazawa, S.-I. and Terashima, I.** (2001) Slow chloroplast development in the evergreen broad-leaved tree species: relationship leaf anatomic characteristics and photosynthetic rate during leaf development. *Plant Cell Environ.* **24**, 279–291.
- Nakhoul, N.L., Davis, B.A., Romero, M.F. and Boron, W.F.** (1998) Effect of expressing the water channel aquaporin-1 on the CO₂ permeability of *Xenopus* oocytes. *Am. J. Physiol.* **274**, C543–C548.

- Nobel, P.S.** (1999) *Physicochemical and Environmental Plant Physiology*, 2nd edn. San Diego: Academic Press.
- Otto, B. and Kaldenhoff, R.** (2000) Cell-specific expression of the mercury-insensitive plasma-membrane aquaporin NtAQP1 from *Nicotiana tabacum*. *Planta*, **211**, 167–172.
- Piel, C., Frak, E., Le Roux, X. and Genty, B.** (2002) Effect of local irradiance on CO₂ transfer conductance of mesophyll in walnut. *J. Exp. Bot.* **53**, 2423–2430.
- Price, D., von Caemmerer, S., Evans, J.R., Yu, J.W., Lloyd, J., Oja, V., Kell, P., Harrison, K., Gallagher, A. and Badger, M.** (1994) Specific reduction of chloroplast carbonic anhydrase activity by antisense RNA in transgenic tobacco plants has a minor effect on photosynthetic CO₂ assimilation. *Planta*, **193**, 331–340.
- Roupsard, O., Gross, P. and Dreyer, E.** (1996) Limitation of photosynthetic activity by CO₂ availability in the chloroplasts of oak leaves from different species and during drought. *Annu. Sci. For.* **53**, 243–254.
- Ruuska, S., Andrews, T.J., Badger, M.R., Hudson, G.S., Laisk, A., Price, G.D. and von Caemmerer, S.** (1998) The interplay between limiting processes in C-3 photosynthesis studied by rapid-response gas exchange using transgenic tobacco impaired in photosynthesis. *Aust. J. Plant Physiol.* **25**, 859–870.
- Santoni, V., Vinh, J., Pflieger, D., Sommerer, N. and Maurel, C.** (2003) A proteomic study reveals novel insights into the diversity of aquaporin forms expressed in the plasma membrane of plant roots. *Biochem. J.* **373**, 289–296.
- Sasaki, H., Samejima, M. and Ishii, R.** (1996) Analysis by delta-13C measurement on mechanism of cultivar difference in leaf photosynthesis on rice (*Oryza sativa* L.). *Plant Cell Physiol.* **37**, 1161–1166.
- Sharkey, T.D., Berry, J.A. and Sage, R.F.** (1988) Regulation of photosynthetic electron-transport in *Phaseolus vulgaris* L., as determined by room-temperature chlorophyll a fluorescence. *Planta*, **176**, 415–424.
- Sharkey, T.D., Savitch, L.V., Butz, N.D.** (1991) Photometric method for routine determination of k_{cat} and carbamylation of rubisco. *Photosynth. Res.* **28**, 41–48.
- Siefritz, F., Tyree, M.T., Lovisolo, C., Schubert, A. and Kaldenhoff, R.** (2002) PIP1 plasma membrane aquaporins in tobacco: from cellular effects to function in plants. *Plant Cell*, **14**, 869–876.
- Singsaas, E.L., Ort, D.R. and De Lucia, E.H.** (2004) Elevated CO₂ effects on mesophyll conductance and its consequences for interpreting photosynthetic physiology. *Plant Cell Environ.* **27**, 41–50.
- Syversten, J.P., Lloyd, J., McConchie, C., Kriedemann, P.E. and Farquhar, G.D.** (1995) On the relationship between leaf anatomy and CO₂ diffusion through the mesophyll of hypostomatous leaves. *Plant Cell Environ.* **18**, 149–157.
- Terashima, I. and Ono, K.** (2002) Effects of HgCl₂ on CO₂ dependence of leaf photosynthesis: evidence indicating involvement of aquaporins in CO₂ diffusion across the plasma membrane. *Plant Cell Physiol.* **43**, 70–78.
- Tournaire-Roux, C., Sutka, M., Javot, H., Gout, E., Gerbeau, P., Luu, D.-T., Bligny, R. and Maurel, C.** (2003) Cytosolic pH regulates root water transport during anoxic stress through gating of aquaporins. *Nature*, **425**, 393–397.
- Tyerman, S.D., Niemietz, C.M. and Bramley, H.** (2002) Plant aquaporins: multifunctional water and solute channels with expanding roles. *Plant Cell Environ.* **25**, 173–194.
- Uehlein, N., Lovisolo, C., Siefritz, F. and Kaldenhoff, R.** (2003) The tobacco aquaporin NtAQP1 is a membrane CO₂ transporter with physiological functions. *Nature*, **425**, 734–737.
- Valentini, R., Epron, D., De Angelis, P., Matteucci, G. and Dreyer, E.** (1995) *In situ* estimation of net CO₂ assimilation, photosynthetic electron flow and photorespiration in Turkey oak (*Quercus cerris* L.) leaves: diurnal cycles under different levels of water supply. *Plant Cell Environ.* **18**, 631–640.
- Van Oosten, J.-J., Wilkins, S. and Besford, R.T.** (1994) Regulation of the expression of photosynthetic nuclear genes by high CO₂ is mimicked by carbohydrates: a mechanism for the acclimation of photosynthesis to high CO₂. *Plant Cell Environ.* **17**, 913–923.
- Volokita, M., Kaplan, A. and Reinhold, L.** (1983) Nature of the rate-limiting step in the supply of inorganic carbon for photosynthesis in isolated *Asparagus sprengeri* mesophyll cells. *Plant Physiol.* **72**, 886–890.
- Warren, C.R. and Adams, M.A.** (2006) Internal conductance does not scale with photosynthetic capacity: implications for carbon isotope discrimination and the economics of water and nitrogen use in photosynthesis. *Plant Cell Environ.* **29**, 192–201.
- Whitney, S.M., von Caemmerer, S., Hudson, G.S. and Andrews, J.T.** (1999) Directed mutation of the Rubisco large subunit of tobacco influences photorespiration and growth. *Plant Physiol.* **121**, 579–588.
- Williams, T.G., Flanagan, L.B. and Coleman, J.R.** (1996) Photosynthetic gas exchange and discrimination against ¹³CO₂ and C¹⁸O¹⁶O in tobacco plants modified by an antisense construct to have low chloroplastic carbonic anhydrase. *Plant Physiol.* **112**, 319–326.
- Ye, Q., Wiera, B. and Steudle, E.** (2004) A cohesion/tension mechanism explains the gating of water channels (aquaporins) in *Chara* internodes by high concentration. *J. Exp. Bot.* **55**, 449–461.